Journal of Physiology (1989), **419**, *pp.* 297–320
With 14 *text-figures*
Printed in Great Britain

THE Mg^{2+} BLOCK AND INTRINSIC GATING UNDERLYING INWARD RECTIFICATION OF THE K^+ CURRENT IN GUINEA-PIG CARDIAC MYOCYTES

BY KEIKO ISHIHARA, TAMOTSU MITSUIYE, AKINORI NOMA AND MAKOTO TAKANO

From the Department of Physiology, Faculty of Medicine, Kyushu University, Fukuoka 812, Japan

(*Received 1 February 1989*)

SUMMARY

1. The blockade by Mg^{2+} and intrinsic gating of the channel, which underlie the rectification of the inward rectifier K^+ current, was investigated using the oil-gap voltage clamp method in isolated guinea-pig ventricular cells.

2. The inward rectifier K^+ current was isolated by subtracting trans-gap currents recorded at an extracellular K^+ concentration ($[K^+]_o$) of 0 mM from those obtained at 14 mM $[K^+]_o$ in the presence of a given concentration of intracellular Mg^{2+} ($[Mg^{2+}]_i$). The reversal potential (V_0) of the difference current was near the equilibrium potential for K^+ (E_K).

3. On repolarization across E_K, the inward rectifier K^+ current showed a rapid exponential increase. The time constant decreased with increasing hyperpolarization, but it was independent of both $[Mg^{2+}]_i$ and the preceding depolarization.

4. When the pre-pulse potential was made progressively positive between V_0-20 and V_0+30 mV, the amplitude of the time-dependent component became larger and the preceding current jump decreased at any $[Mg^{2+}]_i$. With pre-pulses more positive than V_0+40 mV, the time-dependent component started from almost the zero current level at 2 μM $[Mg^{2+}]_i$. At higher $[Mg^{2+}]_i$ (350, 500 and 3000 μM), however, the time-dependent component became smaller as the pre-pulse potential was made more positive than V_0+40 mV.

5. When the membrane was depolarized from a potential of full activation at 2 μM $[Mg^{2+}]_i$, the initial jump in the outward current was ohmic and was followed by an exponential decay. The time-dependent component of the inward current, recorded on repolarization after increasing durations of the preceding depolarization, developed as the outward current decayed. The time constants of both processes were in good agreement.

6. At 500 μM $[Mg^{2+}]_i$, the outward current on depolarization was instantaneously rectified. The time-dependent component recorded on repolarization developed with prolongation of the pre-pulse with a time course slower than at 2 μM $[Mg^{2+}]_i$. The envelope time course became slower as the potential of the depolarization became more positive.

7. Lowering the temperature from 23 to 15 °C slowed the time-dependent current with an apparent Q_{10} of about 3·5 at V_0.

MS 7489

8. Based on the experimental data, kinetic parameters were estimated for a model of Mg^{2+} block, which well simulated the inward-going rectification of the K^+ current.

9. It is concluded that the instantaneous inward rectification on depolarization is due to the Mg^{2+} block at physiological $[Mg^{2+}]_i$. During maintained depolarization, the channels gradually transit from the blocked state to the closed state. The relief of the Mg^{2+} block by repolarization is virtually instantaneous and the time-dependent component of the inward current reflects transition from the closed state to the open state of a gating mechanism.

INTRODUCTION

The inward rectifier K^+ current shows a rapid increase following an instantaneous current jump on repolarization of the membrane. This time-dependent change of the current was ascribed to a gating mechanism which activates with hyperpolarization and deactivates with depolarization in various cells; egg cells (Hagiwara, Miyazaki & Rosenthal, 1976; Hagiwara & Yoshii, 1979), skeletal muscles (Hestrin, 1981; Leech & Stanfield, 1981; DeCoursey, Dempster & Hutter, 1984) and in cardiac myocytes (Kurachi, 1985). This gating kinetics, however, failed to explain the almost instantaneous rectification of the current on depolarization. Additional mechanisms due to single-channel rectification or faster kinetics were expected to be present. Recent studies of the single inward rectifier potassium (K^+) channel in cardiac myocytes revealed that the conductance of the channel in the open state is ohmic, and the outward current through this channel is blocked by physiological concentrations of intracellular Mg^{2+} (Matsuda, Saigusa & Irisawa, 1987; Vandenberg, 1987; Matsuda, 1988). The voltage-dependent Mg^{2+} block was considered as the major mechanism underlying the inward rectification of this channel, as well as for other cardiac K^+ channels (ATP-sensitive K^+ channel, Horie, Irisawa & Noma, 1987; muscarinic K^+ channel, Horie & Irisawa, 1987; Horie & Irisawa, 1989). The single-channel studies also demonstrated that the inward rectifier K^+ channel still closed with time during depolarization in the absence of internal Mg^{2+}, indicating the presence of a voltage-dependent gating mechanism independent of Mg^{2+} block (Matsuda *et al.* 1987; Matsuda, 1988).

With the development of the oil-gap voltage clamp technique (Mitsuiye & Noma, 1987), it was possible to examine effects of intracellular Mg^{2+} on rapid changes of the cardiac inward rectifier K^+ current after voltage jumps under the condition of extensive intracellular perfusion of single myocytes. In the present study, we will demonstrate that the 'activation phase' of the macroscopic current on repolarization is attributable to the intrinsic gating, and that the inward rectification is due to both the Mg^{2+} block and intrinsic gating. A model is proposed which quantitatively describes the contributions of each mechanism to the current changes.

METHODS

Single cell preparation. The procedure of isolating single ventricular cells from the guinea-pig heart was essentially the same as in previous studies (Powell, Terrar & Twist, 1980; Isenberg &

Klöckner, 1982). Briefly, the heart was perfused with a Ca^{2+}-free Tyrode solution containing 0·04% collagenase using a Langendorff-type perfusion system (Imoto, Ehara & Goto, 1985). After the enzyme treatment, the cells were dissociated in KB solution (Isenberg & Klöckner, 1982) and stored in the same solution at 5–7 °C for later use.

Solutions. Tyrode solution contained (in mM): NaCl, 140·0; KCl, 5·4; $CaCl_2$, 1·8; $MgCl_2$, 0·5;

TABLE 1. Internal solutions (mM)

$[Mg^{2+}]_i$ (μM)	Potassium aspartate	KCl	KH_2PO_4	ATP(2K)	EDTA(2K)	HEPES	$MgCl_2$
0	120	20	1	2	5	5	0
2	80	20	1	2	5	5	1·9
350	120	20	1	2	*	5	2·0
500	90	20	1	2	5	5	7·2
3000	90	20	1	2	5	5	10·0

* 2 mM-EGTA was used instead of EDTA in the 350 μM-Mg^{2+} solution.

NaH_2PO_4, 0·33; glucose, 5·5; and the pH was adjusted to 7·4 with 5·0 mM-HEPES–NaOH. The standard Na^+-free external solution contained (in mM); Tris–HCl, 115·0; Tris–base, 20·0; KCl, 14·0; $CaCl_2$, 1·8; glucose, 5·5, and the pH was adjusted to 7·4 by adding HCl. In the K^+-free external solution, KCl was replaced with isomolar Tris–HCl. The compositions of internal test solutions are listed in Table 1. The concentration of free Mg^{2+} in the internal solutions ($[Mg^{2+}]_i$) was calculated using a computer program which was essentially the same as that developed by Fabiato & Fabiato (1979). The absolute stability constants for ethylenediamine tetraacetic acid (EDTA)-Mg, ethyleneglycol-bis-(β-aminoethylether)*N,N'*-tetraacetic acid (EGTA)-Mg and adenosine-5'-triphosphate (ATP)-Mg were those used by Fabiato & Fabiato (1979). The pH of the internal solutions was adjusted to 7·2 by adding KOH and the total K^+ concentration was approximately 140 mM, except in the 350 μM-Mg^{2+} solution in early stages of the present study, where it was 160 mM.

In order to isolate the inward rectifier K^+ current, the Na^+-free external and internal solutions were used to suppress the Na^+ current. The Ca^{2+} current and delayed rectifier K^+ current were negligibly small under the present experimental conditions of extensive internal perfusion. The current records obtained in K^+-free solution were used for subtracting the capacitive and background currents, including the current through the cell membrane within the oil gap.

Oil-gap voltage clamp. The experimental set-up of the oil-gap method is essentially the same as described elsewhere (Mitsuiye & Noma, 1987). It incorporates three compartments for the external solution, the internal solution and the oil gap. The bottom of the compartment for the external solution is made of a cover-glass and the solution is continuously perfused along the free edge of the cover-glass, so that the solution is facing the mineral oil (liquid paraffin, Isizu, Japan) within the gap compartment. The internal compartment is made of a glass pipette with a tip opening of about 0·3 mm. The interior of the glass pipette is continuously perfused with internal solution through a thin-tapered polyethylene tube inserted to near the tip of the glass pipette. Each of the external and internal compartments is mounted on a separate manipulator, so that the width of the oil-gap can be adjusted.

In experiments, a drop of cell suspension was added to the external compartment. The tip of a glass suction pipette was attached to an end of the rod-shaped single myocyte and about two-thirds of the cell was pulled out of the solution into the oil using the suction pipette. Then the internal compartment was moved until the cell end came into contact with the internal solution. The end of the cell was extensively disrupted in the internal solution by crushing with the tip of the suction pipette. Finally, the oil-gap width was adjusted in the range of 30–40 μm.

The same electronic circuitry for voltage clamp incorporated with series resistance compensation was used as described elsewhere (Mitsuiye & Noma, 1987). The external solution was connected to ground through an agar bridge. Before making the bridge of the cell, the internal solution was electrically connected to the external solution by a thin cotton thread. Then, the zero potential of the internal solution was adjusted to a level giving zero current. Under this condition, the liquid junction potential was about -10 mV with reference to the external solution, and all measurements of the membrane potentials were corrected for this value. Experiments were carried out at room

temperature (23 ± 1 °C) except in experiments examining the temperature dependence of the current.

The sealing resistance of the oil gap was determined by assuming a simple equivalent circuit as 30–100 MΩ, which is much larger than the cytoplasmic series resistance of 0·5–0·9 MΩ (Mitsuiye & Noma, 1987). When the cell membrane was exposed to the external K^+-free solution in the present

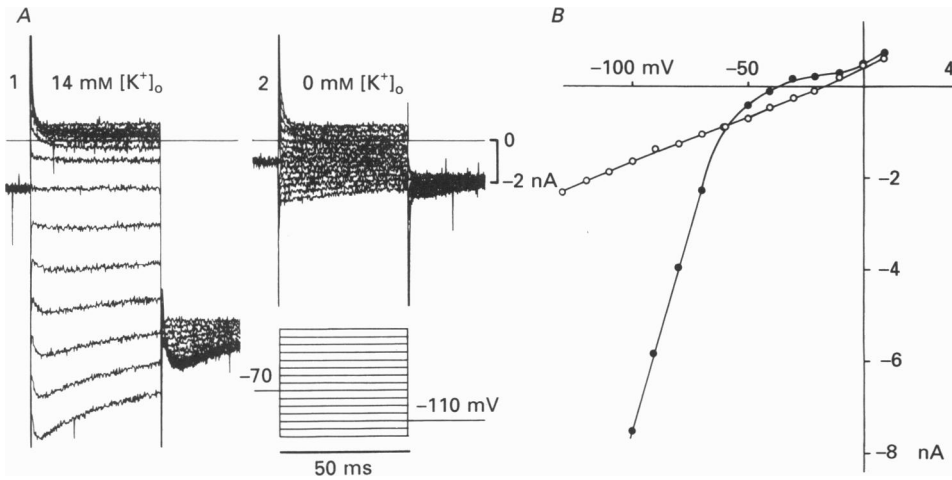

Fig. 1. Suppression of the inward rectifier K^+ current by K^+-free external solution. *A*, current changes elicited by the pulse protocol shown below are superimposed at 14 mM $[K^+]_o$ (1) and 0 mM $[K^+]_o$ (2). $[Mg^{2+}]_i$ was 350 μM. The uppermost trace during the pulse was obtained at +10 mV and the lowermost at −130 mV. The records on repolarization to −110 mV were at −130 mV at the top and at +10 mV at the bottom. The current was sampled at 10 kHz and displayed on a *X–Y* plotter. Horizontal lines indicate the zero current level. *B*, isochronal *I–V* relationships measured near the end of the test pulse at 14 mM $[K^+]_o$ (●) and at 0 mM $[K^+]_o$ (○).

study, a sizeable current was recorded with a maximum slope resistance of 30–100 MΩ (Fig. 1*B*). A large part of this current should have crossed the membrane within the oil gap, since the membrane current is negligibly small in the K^+-free solution as studied by the whole-cell clamp experiment using the patch clamp technique (Matsuda & Noma, 1984). This trans-gap leak current was calculated using a more realistic model of the oil gap, composed of the membrane capacitance and resistance distributed along the oil-gap length (cable theory, Cole & Curtis, 1938; Hodgkin & Rushton, 1946). In the model, the leak current was mostly (> 90%) cancelled by subtracting the current in 0 mM $[K^+]_o$ solution from that in the 14 mM $[K^+]_o$ solution (see Discussion).

Data analysis. Membrane current and potential were recorded on a videotape via a pulse code modulator (PCM-501 modified for DC signal, Sony, Tokyo, Japan), which was incorporated with a 16-bit A/D converter having a fixed sampling interval of 25 μs. Data were analysed by playing back the tape to the memory of a computer (PC-98XL, NEC Tokyo).

RESULTS

Inward rectifier K^+ current isolated as the difference between currents recorded in 14 and 0 mM $[K^+]_o$ solutions

Figure 1*A* shows representative current records obtained in the same cell at 14 and 0 mM $[K^+]_o$. The membrane potential was stepped from a holding potential of −70 mV to various potentials for 50 ms, followed by a second step to −110 mV. At 14 mM $[K^+]_o$ (Fig. 1*A* 1), inward rectification was evident by larger current amplitudes at

voltage steps negative to −60 mV. The activation phase of the inward current was observed at the beginning of hyperpolarizing pulses and slow inactivation of the current followed during large hyperpolarizing pulses. The second voltage step to −110 mV from potentials positive to −70 mV induced activation of the current, followed by marked inactivation (overlapped traces in Fig. 1*A* 1), while the step to −110 mV from more negative potentials induced no time-dependent activation of the current and the amplitude of the current was smaller due to inactivation during the first pulse. These findings are consistent with the hypothesis that there are two separate mechanisms for activation and inactivation, respectively, of the inward rectifier K^+ channel (Ohmori, 1978; Sakmann & Trube, 1984*a*; Biermans, Vereecke & Carmeliet, 1987).

The current changes characteristic for the inward rectifier K^+ current described above almost completely disappeared in the K^+-free external solution (Fig. 1*A* 2), leaving transient outward currents of unknown origin at the onset of strong depolarizations. Their time courses were much faster than the 'transient outward current' described in the whole-cell voltage clamp of isolated cardiac cells (Coraboeuf & Carmeliet, 1982; Josephson, Sanchez-Chapula & Brown, 1984; Nakayama & Irisawa, 1985; Hiraoka & Kawano, 1989).

The isochronal *I–V* relation measured near the end of the first pulse at 0 mM $[K^+]_o$ (Fig. 1*B*, ○) was almost linear. The two *I–V* curves crossed at about −60 mV, which was approximately equal to the potassium equilibrium potential (E_K) calculated from the K^+ concentrations in the external and internal solutions. The reversal potential (V_0) was variable between −50 and −60 mV in other experiments. In the following section, the membrane potential is expressed as the deviation from V_0.

The present study aimed to clarify the mechanism of the activation phase on repolarization of the inward rectifier K^+ current, which was partially obscured by the capacitive current. In Fig. 2, current records are displayed on a fast time scale. Each trace is an average of four current records obtained with clamp pulses of a constant amplitude. Subtraction of the current at 0 mM $[K^+]_o$ including the capacitive current from that at 14 mM $[K^+]_o$ revealed clearly the time-dependent increase of the inward current on repolarization. The initial current jump was negligibly small and the time-dependent current started from almost the zero current level. Close inspection of the difference current revealed a short lag of 80–150 μs between the onset of the pulse and the start of the time-dependent current change of the inward rectifier K^+ current. The lag is most probably due to the delay for the membrane potential to reach the command potential.

When the amplitude of the time-dependent current was measured by extrapolating the fitted exponential curve to time zero, the time zero was arbitrarily set at a point, where the capacitive current decayed to $1/e^2$ of its maximum amplitude.

Comparison of the activation time course between different $[Mg^{2+}]_i$

The time-dependent component of the inward rectifier K^+ current on repolarization shown in Fig. 2 may represent gradual transition from a closed state to open state of the channel gate, or alternatively a time-dependent removal of the Mg^{2+} block. To examine these possibilities, effects of removing $[Mg^{2+}]_i$ on the time-dependent component were tested. The time-dependent component on repolarization was observed regardless of the presence or absence of $[Mg^{2+}]_i$, suggesting an intrinsic

gating mechanism. The quantitative analysis, however, was interfered by the fact that the current became unstable in the complete absence of $[Mg^{2+}]_i$. Thus, the following analysis was performed in the presence of more than 2 μM $[Mg^{2+}]_i$.

Figure 3*A* shows records of the inward current at 2 and 500 μM $[Mg^{2+}]_i$. The

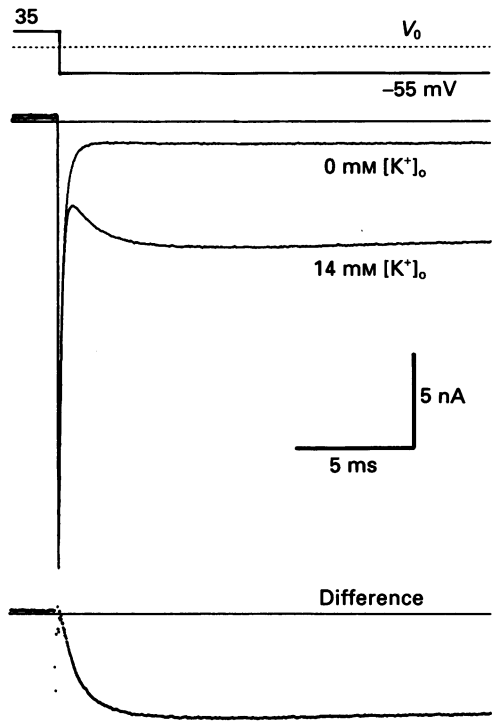

Fig. 2. Isolation of the inward rectifier K^+ current. Average currents of four current records in response to the pulse protocol indicated at the top were obtained at 14 mM $[K^+]_o$ (lower trace) and 0 mM $[K^+]_o$ (upper) and superimposed. The difference between these two currents is shown at the bottom. The potential is given as deviation from the reversal potential V_0. The horizontal line indicates zero current level.

membrane was first depolarized to V_0+35 mV for 40 ms from the holding potential of V_0-35 mV and clamped back to various potentials negative to V_0. All time-dependent currents on repolarization started from near the zero current level in both cases, indicating that the channels were mostly non-conductive, i.e. either in closed or blocked state at the end of the conditioning pulse.

The time course of activation approximated to a single exponential at every test potential, as indicated by the superimposed curve at V_0-35 mV (Fig. 3*A*, right panel). The time constant decreased as the test potential was made more negative. The exponential time constants obtained in seven experiments at 2 μM (left) and 350 or 500 μM $[Mg^{2+}]_i$ (right) were plotted on a logarithmic scale against the potential of the test pulse (Fig. 3*B*). The relationship in each graph was fitted with the following equation by the least-squares method,

$$\tau = K\exp((V_m - V_0)/s), \quad (1)$$

where τ is the time constant, V_m the membrane potential (in mV) and s a slope factor.

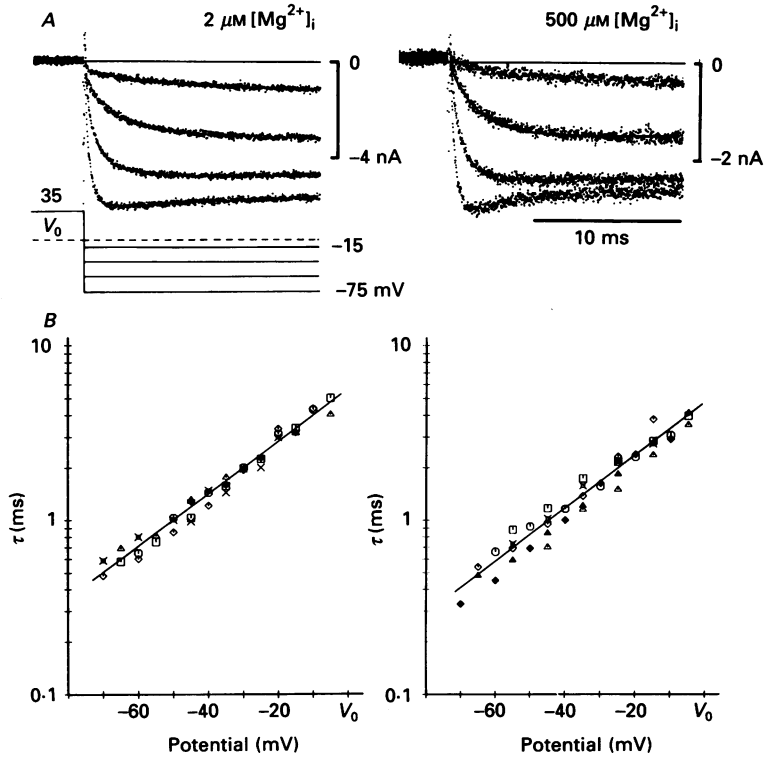

Fig. 3. *A*, time-dependent increase of the inward current on repolarization at 2 μM (left) and 500 μM $[Mg^{2+}]_i$ (right). Difference currents (14 mM $[K^+]_o$ − 0 mM $[K^+]_o$) obtained with four different clamp steps were superimposed. The potential is given as deviation from V_0 in millivolts. The records in the left and right panels were obtained in different cells. The second record from the top in the right panel is fitted with a single-exponential curve. *B*, time constants of the current change plotted against the test potentials. Left, 2 μM; right, 350 (open symbols) and 500 (closed symbols) μM $[Mg^{2+}]_i$. Different symbols indicate different experiments and the straight line is the least-squares fit.

The values of K and s were 5·6 ms and 28·9 mV in the left graph, and 4·7 ms and 28·7 mV in the right graph in Fig. 3*B*. We conclude that the effect of $[Mg^{2+}]_i$ on the time course of the activation phase is minimal.

The values of $K = 5{\cdot}0$ ms and $s = 28{\cdot}8$ mV were obtained from all experimental data. This slope factor is in agreement with 28·7 mV obtained in the same preparation (Saigusa & Matsuda, 1988), but slightly larger than the value reported in the skeletal muscle (18 mV, Leech & Stanfield, 1981) or in the starfish egg (10-fold change per 45–55 mV, Hagiwara *et al.* 1976).

The amplitude of the time-dependent component at various $[Mg^{2+}]_i$ *levels*

To get more insight on the nature of the time-dependent current on repolarization, effects of varying the potential of the preceding depolarization were examined at a low (2 μM) and physiological concentrations of $[Mg^{2+}]_i$ (between 500 and 3000 μM,

Hess, Metzger & Weingart, 1982; Gupta, Gupta & Morre, 1984; Blatter & McGuigan, 1986).

When the membrane was hyperpolarized from a potential negative to V_0-30 mV to more negative potentials, current jump was almost instantaneous (not shown), indicating that the channel is fully activated at potentials more negative to V_0-30

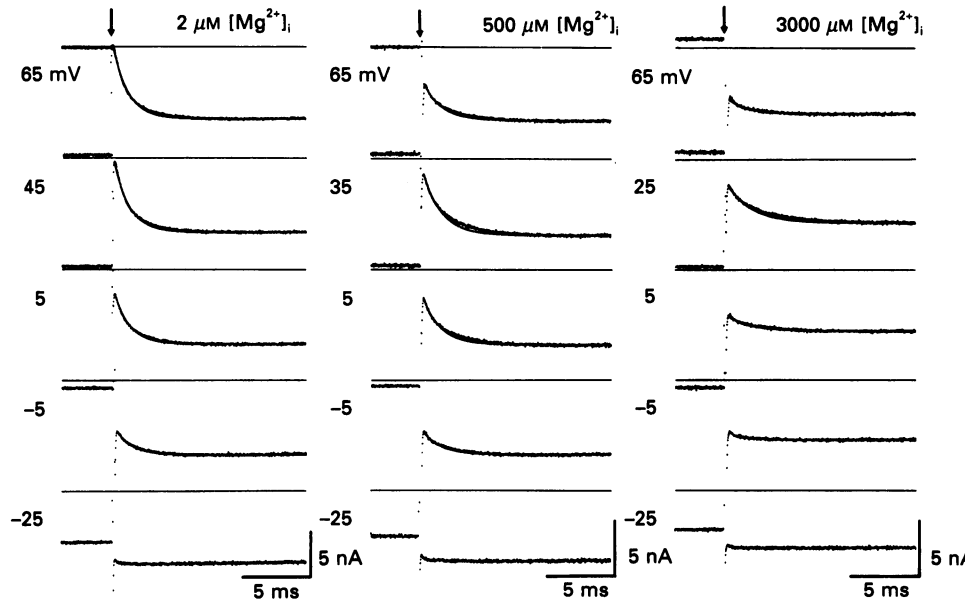

Fig. 4. Dependence of the amplitude of the time-dependent component on both the preceding depolarization and $[Mg^{2+}]_i$. The membrane was depolarized for 40 ms to various levels from the holding potential of V_0-35 mV and clamped back to V_0-35 mV at the time indicated by arrows at 2 (left), 500 (middle) and 3000 μM $[Mg^{2+}]_i$ (right). The numerals at the left of each current record indicate the voltage for the depolarization expressed as a deviation from V_0. Horizontal lines indicate zero current level. Exponential curves were superimposed with time constants of 1·1, 1·3 and 1·6 ms at 2, 500 and 3000 μM $[Mg^{2+}]_i$, respectively. The small notch observed at the beginning of repolarization from a conditioning pulse of V_0-25 mV is of unknown origin. The amplitude of the steady-state inward current decreased as $[Mg^{2+}]_i$ was increased. The background currents in the K^+-free external solution were recorded for subtraction at each $[Mg^{2+}]_i$. All records were obtained in the same experiment lasting approximately one hour.

mV. Figure 4 illustrates the current records on repolarization to V_0-35 mV, following depolarization to various potentials for 40 ms at 2, 500 and 3000 μM $[Mg^{2+}]_i$ in the same cell. The voltage step from V_0-25 mV induced an instantaneous current jump and the time-dependent component was negligibly small. The time-dependent component was induced by repolarization from pre-pulse potentials more positive than V_0-25 mV at every $[Mg^{2+}]_i$. The amplitude of the current change increased with a more positive preceding pulse. At 2 μM $[Mg^{2+}]_i$, the instantaneous current jump became negligibly small with a conditioning pulse more positive than V_0+40 mV. At 500 and 3000 μM $[Mg^{2+}]_i$, however, after reaching a maximum amplitude, the time-dependent component decreased with further depolarization in the preceding pulse.

The averages of the maximum amplitudes of the time-dependent component were obtained at around V_0+35 and V_0+25 mV at 500 and 3000 μM $[Mg^{2+}]_i$, respectively, and were 85·4 ± 5·0 (mean ± S.D., $n = 5$) and 72·3% ($n = 3$) of the plateau amplitude of the inward current at each $[Mg^{2+}]_i$.

Although the amplitude of the time-dependent component was affected, the time course of the current was hardly changed by the potential of the pre-pulse. The time constants used for curve fitting in Fig. 4 were 1·1, 1·3 and 1·6 ms at 2, 500 and 3000 μM $[Mg^{2+}]_i$, respectively. We consider that slight differences in the time constant between different $[Mg^{2+}]_i$ are within the experimental error, because of systematic findings in Fig. 3*B*.

The amplitude of the time-dependent component varied between experiments. In order to demonstrate a general relationship between the amplitude of the time-dependent component and the potential of the depolarizing pre-pulse, measurements in each experiment were normalized to their maximum amplitude at each $[Mg^{2+}]_i$ and were plotted against the pre-pulse potential (Fig. 5). At 2 μM $[Mg^{2+}]_i$, the amplitude of the time-dependent component saturated at potentials positive to V_0+40 mV. At higher $[Mg^{2+}]_i$, the amplitude decreased as the membrane was further depolarized and the extent of the decrease increased with increasing $[Mg^{2+}]_i$. This observation suggests that the decrease of the time-dependent current, or the increase of the instantaneous jump on repolarization, is related to the voltage-dependent Mg^{2+} block of the channel. The time-dependent component may reflect the gating kinetics.

Single-channel analysis of the inward rectifier K^+ channel has shown that internal Mg^{2+} acts as an open-channel blocker (Matsuda, 1988). A reduced kinetic scheme is

$$C \rightleftharpoons O \rightleftharpoons B, \tag{2}$$

where C represents the closed state, O the open state, and B the blocked state of the channel. During depolarization, the channel may be distributed predominantly between states C and B, since the amplitude of the outward current is small. On repolarization, transitions $C \rightarrow O$ and $B \rightarrow O$ may occur, with each rate constant determined by the membrane potential. Based on the above findings, we propose that the removal of Mg^{2+} block on repolarization is almost instantaneous and that the time-dependent component reflects the transition of channels from the closed state to the open state. The relation obtained at 2 μM $[Mg^{2+}]_i$ may represent the gating kinetics under minimal influence of Mg^{2+} block.

The time- and voltage-dependent decay of the outward current at 2 μM $[Mg^{2+}]_i$

To test the above hypothesis, we analysed first the current obtained at 2 μM $[Mg^{2+}]_i$, which may be free from Mg^{2+} block. When the membrane was depolarized from a potential of full activation (V_0-65 mV) to potentials positive to V_0, time-dependent decay of the outward current was observed as shown in Fig. 6*A*. The rising phase of the outward current was due to an artifact of the subtraction procedure. Neglecting this phase, the decay time course was fitted with a single exponential curve as shown in the inset of Fig. 6*B*. The 'instantaneous' current levels in Fig. 6*A* were obtained by extrapolating the exponential curve to time zero (Fig. 6*B*, ○). The data points were fitted with a straight line, which was extrapolated from the isochronal (15 ms) *I–V* relation of the inward current (●). The plot of the time

constants of the outward current at different potentials clearly showed voltage dependence of the kinetics (Fig. 6*C*, open symbols).

The relationship between the time course of the outward current during depolarization and development of the time-dependent current on repolarization was

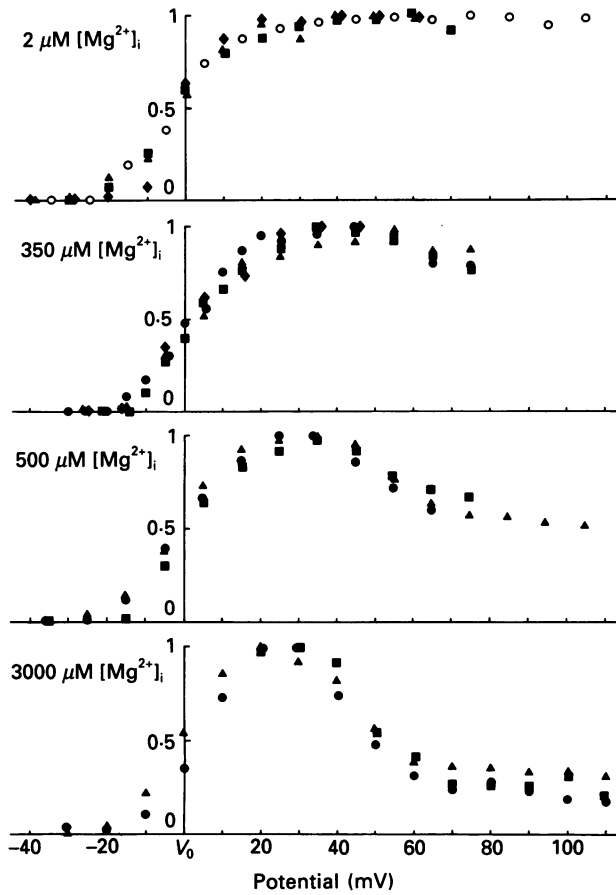

Fig. 5. Normalized amplitude of the time-dependent component plotted against the preceding potential at different $[Mg^{2+}]_i$. The unit amplitude on the ordinate corresponds to about 85 and 72 % of the steady-state inward current at 350–500 and 3000 μM $[Mg^{2+}]_i$. Data at 2, 500 and 3000 μM $[Mg^{2+}]_i$ were obtained with 40 ms pre-pulse, except those indicated with open symbols at 2 μM $[Mg^{2+}]_i$, which were obtained with a 500 ms pre-pulse. Data at 350 μM $[Mg^{2+}]_i$ were obtained with a 50 ms pre-pulse. Different symbols indicate different experiments: four, five, three and three experiments at 2, 350, 500 and 3000 μM $[Mg^{2+}]_i$, respectively.

examined. The membrane potential was first clamped to V_0-35 mV for channel activation and then depolarized to V_0+15 mV or V_0+45 mV for various durations and finally repolarized to V_0-35 mV (Fig. 7*A*). The amplitude of the time-dependent inward current increased as the depolarizing pulse was prolonged. Each time-dependent component at V_0-35 mV could be fitted with a time constant of 1·0 ms. The amplitude of the time-dependent component was normalized (i) referring to their maximum amplitude and values of ($1-i$) were plotted against the duration of

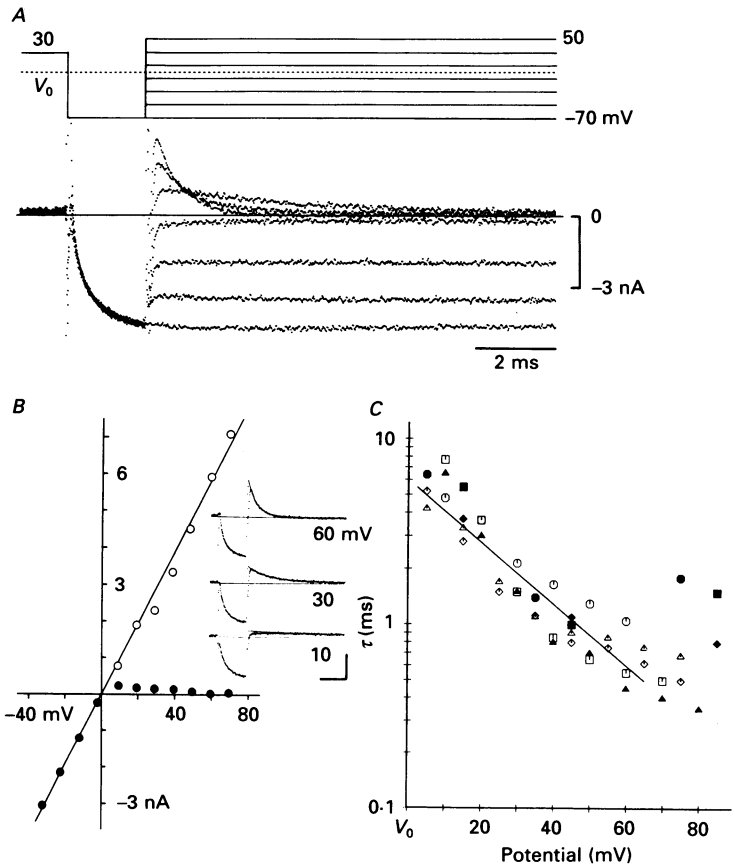

Fig. 6. The time-dependent outward current on depolarization at 2 μM $[Mg^{2+}]_i$. *A*, the currents elicited by the pulse protocol shown on the top are superimposed. The difference current showed a rapid upward deflection at the beginning of the depolarizing pulse. We assume that this is an artifact of subtraction caused by fluctuations of the transient outward current of unknown nature (see Fig. 1*A* 2). *B*, *I–V* relations measured 15 ms after the onset of the second pulse (●) and that estimated by extrapolating the exponential time course to time zero (○) as shown in the inset. Numbers in the inset indicate the potential deviation from V_0 (in mV) during the test pulse. Calibrations, 2 ms and 3 nA. *C*, open symbols: time constants of the outward current decay plotted against the potential of the second pulse in four experiments. The straight line is the least-squares fit to data points over the potential range negative to V_0+60 mV. Closed symbols: the time constants obtained by the envelope test (Fig. 7) in four experiments plotted against the potentials of depolarizing pulse.

the conditioning depolarization in Fig. 7*B* (envelope test). The line fitting gave a time constant of 3·7 ms at V_0+15 mV and 1·0 ms at V_0+45 mV, respectively. These values are nearly equal to time constants of the corresponding outward current decay, which were 4·0 ms at V_0+15 mV and 0·9 ms at V_0+45 mV.

The time constants of the envelope were plotted against the potential of the depolarizing pulse in Fig. 6*C* (closed symbols) and were compared with those of the

outward currents (open symbols). It is evident that the time course of the envelope agrees well with that of the time-dependent outward current over the potential range from V_0 to V_0+60 mV. These findings are consistent with the view that the current changes reflect intrinsic gating at 2 μM $[Mg^{2+}]_i$, at least over the potential range negative to V_0+60 mV. The line drawn in Fig. 6*C* was determined by the least-squares fit of eqn (1) over the potential range negative to V_0+60 mV: $K = 6{\cdot}0$ ms and $s = -25{\cdot}8$ mV.

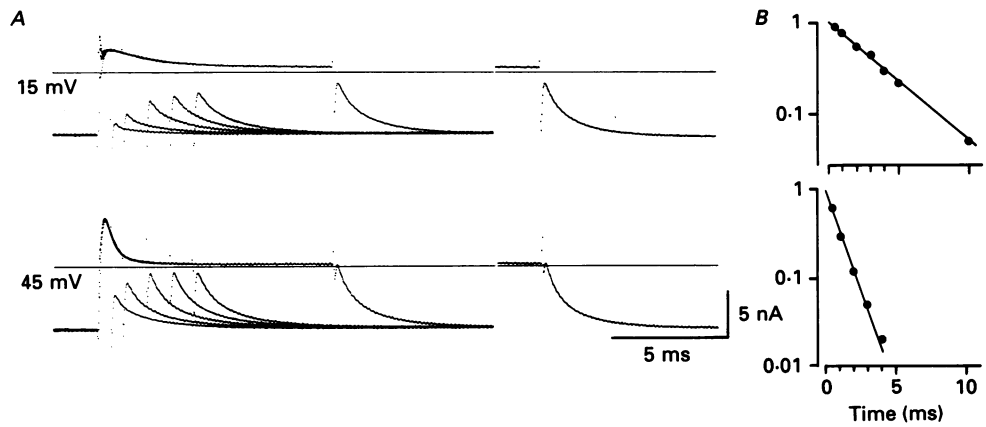

Fig. 7. The envelope test of the time-dependent component at 2 μM $[Mg^{2+}]_i$. *A*, currents elicited by repolarization to V_0-35 mV after various durations (0·5, 1, 2, 3, 4 and 10 ms) of depolarizing pulse to V_0+15 (upper) and V_0+45 mV (lower) are superimposed. The currents on the right were obtained with 100 ms depolarizing pre-pulses. The time constants of the outward current decay during the maintained depolarization were 4·0 ms at +15 mV and 0·9 ms at +45 mV. *B*, the amplitudes of the time-dependent current were normalized to their maximum amplitude and were plotted against the duration of the preceding pulse. The straight lines fitted give time constants of 3·7 and 1·0 ms, respectively.

At V_0+70 and V_0+80 mV, the time course of the envelope seemed to be slower than that of the outward current and it was not fitted with a single-exponential function. For practical purpose, the time giving the amplitude of $1-e^{-1}$ of the steady-state amplitude was estimated and plotted in Fig. 6*C*. This finding may suggest an influence of the Mg^{2+} block on the envelope time course on strong depolarization even at 2 μM $[Mg^{2+}]_i$.

Mg^{2+} block of the inward rectifier K^+ current at 500 μM $[Mg^{2+}]_i$

At 500 μM $[Mg^{2+}]_i$, the rectification was almost instantaneous and the fast time-dependent decay observed at 2 μM $[Mg^{2+}]_i$ (Fig. 6) was hardly seen in the outward current (Fig. 8*A*). This effect of $[Mg^{2+}]_i$ was reversible as shown in Fig. 8*B*, where the 500 μM $[Mg^{2+}]_i$ and 2 μM $[Mg^{2+}]_i$ solutions were applied alternately while the same pulse protocol was repeated. The time-dependent outward current at 2 μM $[Mg^{2+}]_i$ developed several minutes after switching the internal solution. The time lag was attributed to delayed exchange of the internal solution in the perfusing tube. The instantaneous rectification of the outward current on depolarization may indicate

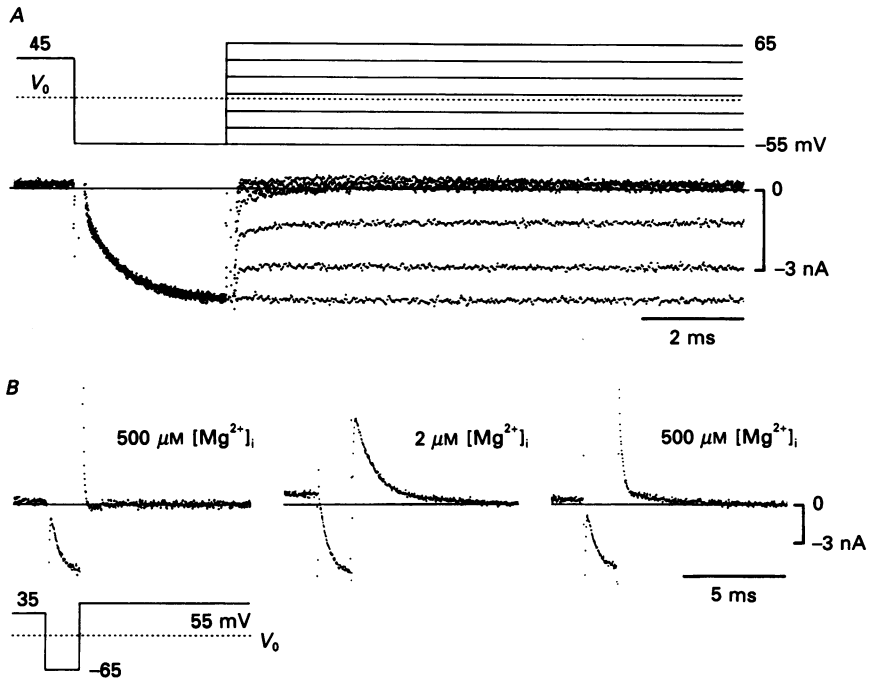

Fig. 8. *A*, the current records obtained at 500 μM $[Mg^{2+}]_i$ with the pulse protocol indicated. Note that the time-dependent outward current observed at 2 μM $[Mg^{2+}]_i$ in Fig. 6*A* is absent at 500 μM $[Mg^{2+}]_i$. *B*, typical current records obtained by applications of 500, 2 and 500 μM $[Mg^{2+}]_i$ solutions in sequence. The spikes at the beginning of the currents on depolarization (500 μM) are due to subtraction artifacts. The pulse protocol is shown at the bottom.

that the channel is blocked immediately after the onset of depolarization at 500 μM $[Mg^{2+}]_i$.

The envelope time course of the time-dependent current on repolarization was measured as shown in Fig. 9*A*. When the duration of the preceding depolarization was short, the current change on repolarization was dominated by the instantaneous component in accordance with the view that the channel is instantaneously relieved from the Mg^{2+} block on repolarization (B → O transition in eqn (2)).

When the duration of the conditioning depolarization was prolonged, however, the envelope test revealed slow development of the time-dependent component in expense of the instantaneous component. The time constant of individual time-dependent component remained constant (1·5 ms) regardless of the duration of the preceding depolarization. The envelope time course was not single exponential. The time to reach $1-e^{-1}$ of the steady-state amplitude was plotted against the potential of conditioning depolarization in Fig. 9*B*. The values were larger than those at 2 μM $[Mg^{2+}]_i$ and they increased with depolarization. This voltage dependence is in contrast to that of the time constant at 2 μM $[Mg^{2+}]_i$. The finding may be explained by assuming that the channels are firstly blocked on depolarization, and then slowly

redistributed between closed states and blocked states according to an equilibrium proportion determined by both the gating and blocking kinetics (see Discussion for a more quantitative description).

The above experimental observations indicate that the voltage relation of the

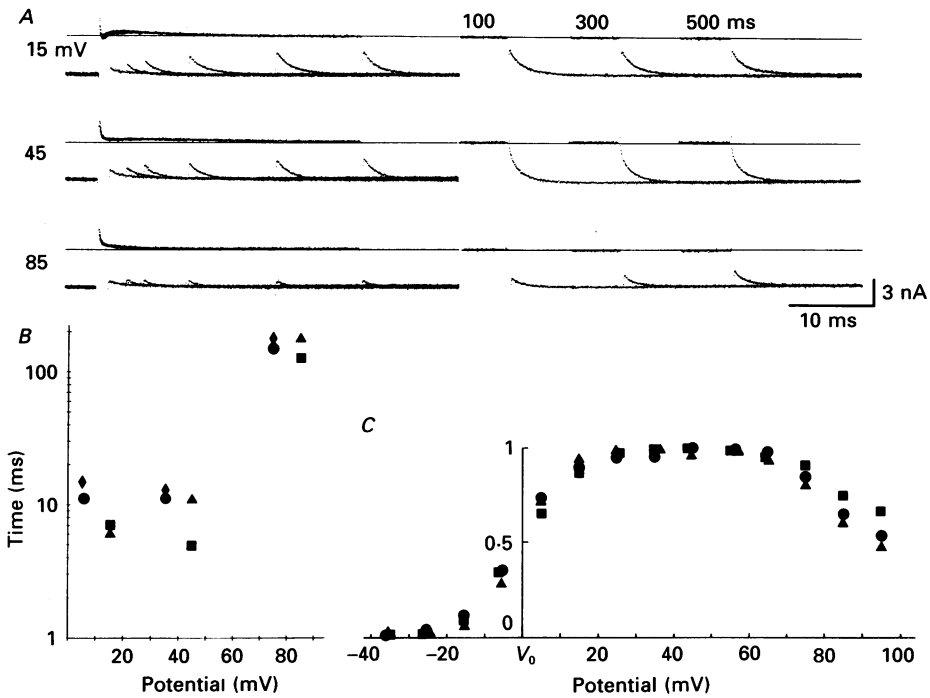

Fig. 9. *A*, the envelope test at 500 μM $[Mg^{2+}]_i$. Essentially the same pulse protocol as in Fig. 7 was used. Numerals indicate potentials during depolarization in reference to V_0. Current records obtained with 1, 3, 5, 10, 20 and 30 ms depolarizing pulses are superimposed in the left half of the panel and those with 100, 300 and 500 ms pulses are illustrated on the right. The spikes at the beginning of the currents on depolarization are due to subtraction artifacts. *B*, times to reach $1-e^{-1}$ of the steady-state amplitude are plotted against the potentials of the depolarizing pulse in four experiments. *C*, the voltage relation of the amplitude of the time-dependent component at 500 μM $[Mg^{2+}]_i$ determined as in Fig. 5, but using a 500 ms pre-pulse.

amplitude of the time-dependent component in Fig. 5 is influenced by the duration of the conditioning pulse. Therefore, the steady-state probability of the closed state at 500 μM $[Mg^{2+}]_i$ was re-evaluated using a depolarizing pulse of 500 ms in duration (Fig. 9*C*). The maximum amplitude thus obtained was nearly 100% of the steady-state inward current. Over the potential range negative to V_0+50 mV, the relation was almost superposable to that determined at 2 μM $[Mg^{2+}]_i$ (Fig. 5). It should be noted that in case of 2 μM $[Mg^{2+}]_i$, the relationship obtained with pre-pulse of 500 ms was superposable with those obtained with 40 ms pre-pulse (Fig. 5).

Effects of temperature on the time-dependent component

The intrinsic gating mechanism of the channel may have a high temperature dependence. To confirm the gating mechanism underlying the time-dependent

current component on repolarization, the effects of lowering the temperature from 23 ± 1 to 15 ± 1 °C were examined at 500 μM $[Mg^{2+}]_i$.

The membrane was repolarized to $V_0 - 35$ mV following depolarization to various potentials for 100 ms (Fig. 10*A*). The time-dependent component was single

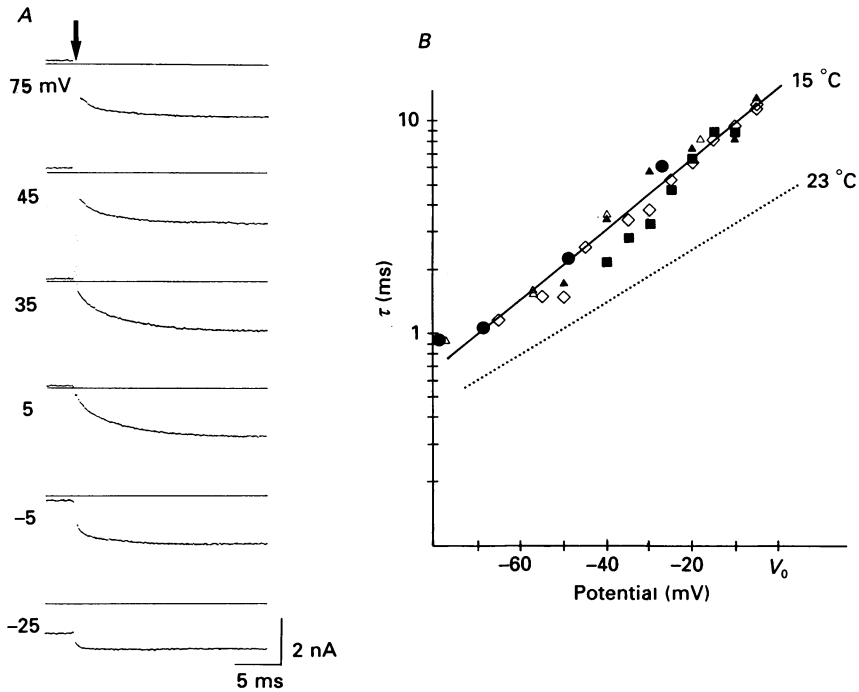

Fig. 10. The effect of temperature on the time-dependent current. *A*, current records obtained with pulse protocol shown at the bottom at 15 °C. Duration of the preceding pulses was 100 ms and $[Mg^{2+}]_i$ was 500 μM. *B*, the voltage dependence of the time constant of the activation phase determined at 15 °C by using a pulse protocol similar to that shown in Fig. 3. Different symbols indicate different experiments and the continuous line is the least-squares fit. The dotted line is drawn according to the voltage dependence at 23 °C in Fig. 3*B* for comparison.

exponential, but its rate was obviously slower than that obtained at room temperature. The proportion of the time-dependent component to the steady-state inward current increased with increasing depolarization during the conditioning pulse at potentials negative to $V_0 + 35$ mV and decreased with further depolarization.

The exponential time constants were plotted against the test potentials on a semilogarithmic scale in Fig. 10*B*. The least-squares fitting eqn (1) gave values of $K = 14{\cdot}3$ ms and $s = 25{\cdot}5$ mV. We consider that the difference of the slope between 23 and 15 °C is within the range of experimental error. The Q_{10} calculated at V_0 was 3·50. This is in agreement with previous studies in other tissues (Hagiwara & Yoshii, 1980; Leech & Stanfield, 1981).

DISCUSSION

Isolation of the inward rectifier K^+ current

The inward rectifier K^+ current was measured as the difference between records obtained at 14 mM $[K^+]_o$ and those obtained in the K^+-free solution, as has been done previously (Saigusa & Matsuda, 1988). This method is justified by the fact that the inward rectifier K^+ current disappears at zero $[K^+]_o$, resulting in an almost linear I–V relation in the steady state (Ohmori, 1978; Matsuda & Noma, 1984). The reversal potential of the difference current was near the calculated E_K and the changes in the I–V curve observed by depleting $[K^+]_o$ (Fig. 1) were quite similar to those observed by suppressing the inward rectifier using high concentrations of channel blockers, such as Cs^+ or Ba^{2+} (Isenberg, 1976; Mitsuiye & Noma, 1987).

To estimate an error introduced in subtracting the leak current, the current in the oil gap was calculated using a computer model. We used the equivalent circuit of the cell membrane composed of membrane capacitance C_m and resistance R_m, which were distributed along the length of the oil gap together with the intracellular axial resistance R_i and the extracellular sealing resistance R_e (Cole & Curtis, 1938; Hodgkin & Rushton, 1946). This model is more realistic than the simple equivalent circuit, having only R_i and R_e in the gap used in the previous study (Mitsuiye & Noma, 1987). A linear gradient from 140 mM (internal solution) to 14 or to 0 mM (external solution) was assumed in $[K^+]_o$ in the narrow extracellular space in the oil. According to this $[K^+]_o$ gradient, E_K should continuously alter along the gap. If the membrane conductance is mostly determined by the inward rectifier K^+ channel in our experiment, R_m would also change. The conductance of the inward rectifier K^+ channel was assumed to be proportional to the 0·62th power of $[K^+]_o$ (Sakmann & Trube, 1984*b*). We used eqn (7) to describe the open probability of the K^+ channels as a function of $(V_m - E_K)$.

The values used were: R_m, 0·02 MΩ/cm at 5·4 mM $[K^+]_o$; R_i, 104 MΩ/cm; R_o in the gap, 17500 MΩ/cm (Mitsuiye & Noma, 1987). The computation started with a given membrane potential at the end of the cell in the external compartment. It calculated the membrane currents through R_m, R_i, and R_e in sequential segments of less than 0·2 μm in length from the end towards the internal compartment, and determined the amplitude of trans-gap current, which must be applied through the oil gap to maintain the given potential. The two trans-gap current–voltage relations (circles in Fig. 11) thus obtained well simulated the experimental I–V curves (Fig. 1) in the K^+-free and 14 mM $[K^+]_o$ solutions. The difference between the two curves was almost equal to the K^+ current in the 14 mM $[K^+]_o$ external compartment (triangles) within an error range of less than 10%. This is because profiles of both the membrane potential and E_K in the oil gap are similar between the two conditions, except in the portion very near to the interface between oil and the external compartment.

The thickness of the water layer, separating the cell membrane and oil in the gap, was estimated to be about 12 nm based on the specific resistivity of saline and the seal resistance (Mitsuiye & Noma, 1987). Within this narrow extracellular space, the transmembrane K^+ current might change $[K^+]_o$. In the above model calculation, the K^+ current density was at most 1·9 pA/μm², which might change $[K^+]_o$ at a rate of 1·7 mM/ms. However, this effect is limited only in the gap region near the interface

between the oil and external compartment. The current density becomes progressively smaller and $[K^+]_o$ increases toward the internal compartment. Thus, the limited extracellular space might not alter the time course of the leak current during several milliseconds, during which the time-dependent change of the inward rectifier

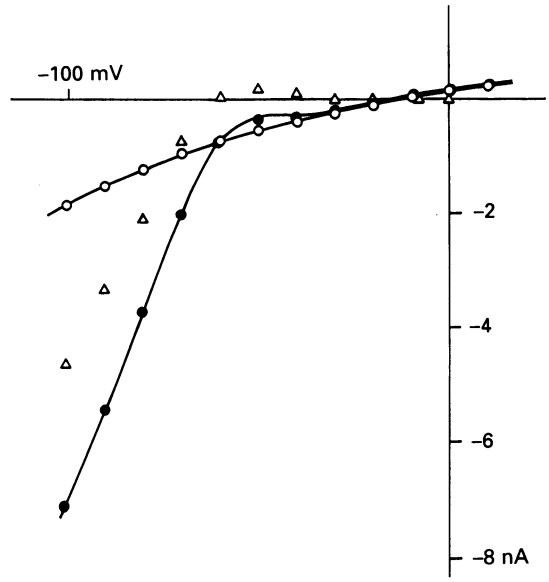

Fig. 11. Simulation of the trans-gap current–voltage relations using a cable model: ●, 14 mM $[K^+]_o$; ○, 0 mM $[K^+]_o$. The K^+ currents through the cell membrane in both the external solution and the oil gap were calculated based on the cable theory. △, the current flow through the membrane in the external solution at 14 mM $[K^+]_o$.

K^+ current was examined. In fact, the current record did not show clear time-dependent changes on hyperpolarization in the K^+-free solution.

The time-dependent component of the inward current reflects channel activation

On repolarization to potentials negative to V_0, the difference current showed an instantaneous jump, followed by a time-dependent increase in the inward current. In this study, we attributed the time-dependent component to the transition of the channel from state C to O in scheme (2) according to the following findings. (1) The time course of the time-dependent component was neither affected by varying $[Mg^{2+}]_i$ nor by varying the amplitude and duration of the preceding depolarization. (2) The amplitude of the time-dependent component on repolarization was decreased by increasing $[Mg^{2+}]_i$. In contrast, the size of the instantaneous current jump on repolarization following depolarization ($> V_0 + 40$ mV) was increased by increasing both $[Mg^{2+}]_i$ and the preceding depolarization. The relief from the Mg^{2+} block by repolarization was concluded to be instantaneous. (3) The value of Q_{10} (3·5) obtained for the time constant of the time-dependent component is in good agreement with the temperature dependence of the gating kinetics of various ionic channels (Hodgkin, Huxley & Katz, 1952; Frankenhaeuser & Moore, 1963).

Intrinsic gating

The activation kinetics of the inward rectifier was described by the first-order kinetics in the egg cell (Hagiwara *et al.* 1976), skeletal muscle (Leech & Stanfield, 1981) and cardiac myocyte (Kurachi, 1985). The present study also showed exponential activation phase in the inward rectifier K^+ current. The first-order kinetics for the activation gate is described as

$$C \underset{\beta}{\overset{\alpha}{\rightleftharpoons}} O, \tag{3}$$

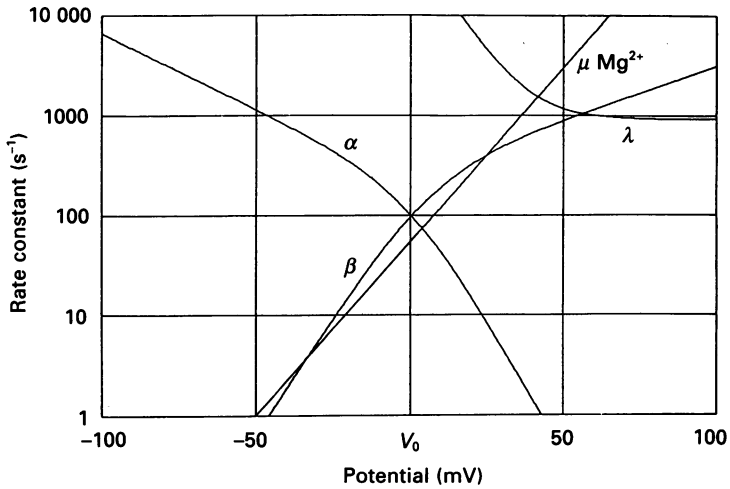

Fig. 12. The rate constants for the opening (α) and closing (β) of the activation gate and for unblocking of the Mg^{2+} block (λ). The blocking rate (μ Mg^{2+}) is given at 500 μM $[Mg^{2+}]_i$.

where α and β are the rate constants. The steady-state probability of state O, P_O, and the time constant for the current change (τ) are,

$$P_O = \alpha/(\alpha+\beta), \tag{4}$$

and

$$\tau = (\alpha+\beta)^{-1}. \tag{5}$$

The steady-state probability of state C (P_C) was experimentally determined from the time-dependent component–voltage relation at 2 μM $[Mg^{2+}]_i$ in Fig. 5. Then,

$$P_O = 1-P_C. \tag{6}$$

The equation, which simulates the experimental data is,

$$P_O = (1+\exp((V_m-V_0)/6{\cdot}8)^{-1}. \tag{7}$$

Values for α and β were calculated from experimental eqns (1) and (7) using eqns (4) and (5). Their voltage relations were described as (Fig. 12)

$$\alpha(s^{-1}) = 200\exp[-0{\cdot}035(V_m-V_0)]/\{\exp[0{\cdot}088(V_m-V_0)]+1\}, \tag{8}$$

$$\beta(s^{-1}) = 300\exp[0{\cdot}11(V_m-V_0-6)]/\{\exp[0{\cdot}085(V_m-V_0-6)]+1\}. \tag{9}$$

Blocking kinetics

The single-channel analysis revealed that the inward rectifier K^+ channel is composed of three identical conducting subunits and each subunit is blocked by Mg^{2+} independently. Therefore, the kinetics of the Mg^{2+} block of the inward rectifier K^+ channel was described as follows (Matsuda, 1988):

$$C \underset{\beta}{\overset{\alpha}{\rightleftharpoons}} O \underset{\lambda}{\overset{3\mu Mg^{2+}}{\rightleftharpoons}} B_1 \underset{2\lambda}{\overset{2\mu Mg^{2+}}{\rightleftharpoons}} B_2 \underset{3\lambda}{\overset{\mu Mg^{2+}}{\rightleftharpoons}} B_3, \tag{10}$$

where B_1, B_2 and B_3 indicates one, two and all of the elementary channels blocked by intracellular Mg^{2+}, respectively and μ indicates a second-order rate constant for blocking and λ an unblocking rate constant. In the steady state,

$$\alpha P_C = \beta P_O, \tag{11}$$

$$(\beta + 3\mu\ Mg^{2+}) P_O = \alpha P_C + \lambda P_{B1}, \tag{12}$$

$$(\lambda + 2\mu\ Mg^{2+}) P_{B1} = 3\mu\ Mg^{2+} P_O + 2\lambda P_{B2}, \tag{13}$$

$$(2\lambda + \mu\ Mg^{2+}) P_{B2} = 2\mu\ Mg^{2+} P_{B1} + 3\lambda P_{B3}, \tag{14}$$

$$3\lambda P_{B3} = \mu\ Mg^{2+} P_{B2}, \tag{15}$$

$$P_C + P_O + P_{B1} + P_{B2} + P_{B3} = 1. \tag{16}$$

From above equations, the following relation was obtained:

$$K_B = (K_G / P_C - K_G)^{\frac{1}{3}} - 1, \tag{17}$$

where K_G and K_B represent β/α and $\mu\ Mg^{2+}/\lambda$, respectively. Representative values of K_B were calculated from eqns (8) and (9), and P_C, which was obtained at 500 μM $[Mg^{2+}]_i$ in Fig. 9*C*. The voltage relation of K_B was fitted by an equation,

$$K_B = 0{\cdot}06 \exp((V_m - V_0)/12{\cdot}5). \tag{18}$$

The dissociation constant for Mg^{2+} block (given as the reciprocal of K_B) was about 20–30 μM at $V_0 + 70$ mV, which is larger by about one order of magnitude than that obtained from the single-channel recordings (1·7 μM; Matsuda, 1988).

Since the values of μ and λ were not obtained directly in the present study, we referred to the measurements in the single-channel study as follows. Because λ seems to be voltage independent over the potential range between $E_K + 50$ and $E_K + 90$ mV (Matsuda, 1988, see also, Horie *et al.* 1987), we attributed the voltage dependence of K_B to that of μ. Then, μ and λ in the present study were obtained by adopting the value of μ at $E_K + 70$ mV in the single-channel analysis (3×10^7 M^{-1} s^{-1}). The rate constants are,

$$\mu\ (M^{-1}\ s^{-1}) = 110000 \exp((V_m - V_0)/12{\cdot}5), \tag{19}$$

$$\lambda\ (s^{-1}) = 920. \tag{20}$$

To simulate the instantaneous unblocking on repolarization, we tentatively modified the eqn (20) for λ,

$$\lambda\ (s^{-1}) = 920 + 50000 \exp((V_m - V_0)/(-9{\cdot}5)). \tag{21}$$

The voltage relations of these rate constants are illustrated in Fig. 12.

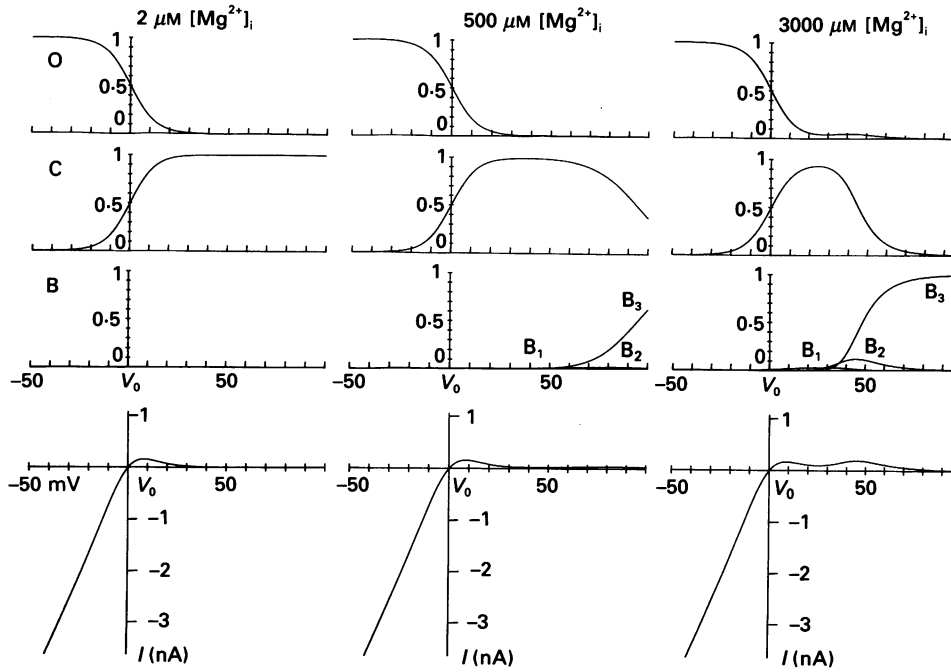

Fig. 13. Reconstructed voltage dependence of the probabilities for open (O), closed (C), and blocked (B) states of the channel and I–V relations in the steady state. Left column, 2 μM, middle, 500 μM and right, 3000 μM $[Mg^{2+}]_i$. B_1, B_2 and B_3 are defined by eqn (10). Amplitude of the current is given in arbitrary units.

Reconstruction of the K^+ current

By using the above rate constants, we reconstructed the voltage relations of steady-state probabilities of states O, C, B_1, B_2 and B_3 at 2, 500 and 3000 μM $[Mg^{2+}]_i$ in Fig. 13. The voltage relation of the time-dependent current shown in Fig. 5 (2 μM $[Mg^{2+}]_i$) and in Fig. 9C (500 μM $[Mg^{2+}]_i$) were well simulated: P_C at potentials negative to $V_0 + 30$ mV was not markedly affected by $[Mg^{2+}]_i$, and it decreased with strong depolarization in the presence of higher $[Mg^{2+}]_i$. This model successfully revealed the voltage-dependent increase of P_B at the expense of P_C.

The conductance of states B_1 and B_2 are $\frac{2}{3}$ and $\frac{1}{3}$ of that in the full open state, respectively. Thus, the macroscopic conductance generated by the inward rectifier K^+ channel is given as,

$$G = \gamma N(P_O + \tfrac{2}{3}P_{B1} + \tfrac{1}{3}P_{B2}), \quad (21)$$

where γ and N are the single-channel conductance and the total number of channels of a single cell, respectively. In the lower panel of Fig. 13, the reconstructed steady-state I–V relations at 2, 500 and 3000 μM $[Mg^{2+}]_i$ are shown. These curves show inward rectification at the potentials above V_0.

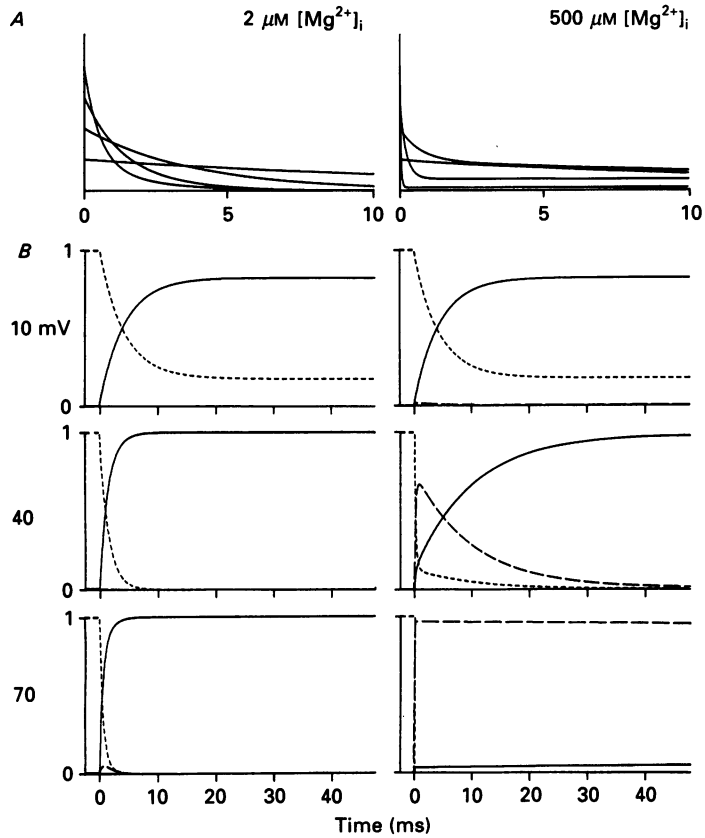

Fig. 14. *A*, reconstructed time course of the outward currents on depolarizations to V_0+20, $+40$, $+60$ and $+80$ mV from a holding potential of V_0-40 mV. *B*, probability of open (dotted line), closed (continuous line) and blocked states (dashed line) of the channel on depolarization. The voltage steps from V_0 are indicated on the left. Time zero indicates the onset of the depolarizing step from V_0-40 mV. Left column, 2 μM, right, 500 μM $[Mg^{2+}]_i$.

The time-dependent current changes on depolarizations to V_0+20, 40, 60 and 80 mV from V_0-40 mV are reconstructed at 2 and 500 μM $[Mg^{2+}]_i$ in Fig. 14*A*. The changes in the distribution of the channel states at V_0+10, 40 and 70 mV are shown in *B*, which may correspond to the experimental findings in Figs 7 and 9. The time course of the decay of the outward current at 500 μM $[Mg^{2+}]_i$ is much faster than at 2 μM $[Mg^{2+}]_i$. At 2 μM $[Mg^{2+}]_i$, the time-dependent current change is simply due to a

transition from state O to C. In the presence of 500 μM $[Mg^{2+}]_i$, a certain fraction of channels are first blocked by Mg^{2+} on depolarization and then gradually transit through O to C during the maintained depolarization. The transition to C is much slower than at 2 μM $[Mg^{2+}]_i$ and becomes even slower as the potential is made more positive. These time courses are in agreement with the results of the envelope tests (Fig. 9).

Inconsistency of the model

Although most of the experimental data in the present study were described by the model given by eqn (10), a few problems remain. The instantaneous rectification in the outward current on small depolarization to V_0+5 or $+25$ mV (Fig. 8) was not simulated by the model (Fig. 14). It could be simulated only if we use a larger blocking rate constant estimated from the voltage dependence in the single-channel analysis. However, in this case virtually no outward current was generated in the steady state, because most of the channels are trapped in state B_3.

The rectification of the steady-state *I–V* curve in this model was steeper than the *I–V* curves reported in cardiac myocytes: the outward component of the inward rectifier K^+ current is more prominent (Isenberg, 1976; Matsuda & Noma, 1984). The extent of the rectification in this model is determined mainly by the voltage relation of the activation parameter. The steady-state activation measured in our study, however, is quite similar to those obtained using different techniques in the same preparation (Kurachi, 1985; Saigusa & Matsuda, 1988).

The blocking and unblocking rate constants in the model are different from those obtained from the single-channel analysis. If the smaller unblocking rate constant obtained from the single-channel analysis was used in the model, transition from state B to O hardly occurred during depolarization at 500 μM $[Mg^{2+}]_i$: P_C in the steady state at $+50$ or 70 mV was less than 0·01, when α and β in eqns (8) and (9) were used. This is in contrast to the findings shown in Fig. 9. We have, at present, no clear explanation for the differences in the rate constants for blocking kinetics between the macroscopic current and the single-channel current analysis. It is possible that the gating and the blocking kinetics of the channel are modulated by the experimental conditions. For example, the $[K^+]_o$ used in the present study is different from that in the single-channel analysis. The extent of the internal perfusion may also be different among the oil-gap method, the open cell-attached configuration and the excised patch recordings. It should be noted that estimations of rate constants in the present study are all based on a particular model. A different type of the model might give better explanations.

We thank Dr T. Powell and Dr H. Matsuda for useful comments on the manuscript and Fumiko Katsuda for secretarial services. This work was supported by Grants in Aid for Scientific Research from the Ministry of Education, Science and Culture of Japan.

REFERENCES

BIERMANS, G., VEREECKE, J. & CARMELIET, E. (1987). The mechanism of the inactivation of the inward-rectifiying K current during hyperpolarization steps in guinea-pig ventricular myocytes. *Pflügers Archiv* **410**, 604–613.

BLATTER, L. A. & MCGUIGAN, J. A. S. (1986). Free intracellular magnesium concentration in ferret

ventricular muscle measured with ion selective micro-electrodes. *Quarterly Journal of Experimental Physiology* **71**, 467–473.

COLE, K. S. & CURTIS, H. J. (1938). Electric impedance of *Nitella* during activity. *Journal of General Physiology* **22**, 37–64.

CORABOEUF, E. & CARMELIET, E. (1982). Existence of two transient outward currents in sheep cardiac Purkinje fibers. *Pflügers Archiv* **392**, 352–359.

DECOURSEY, T. E., DEMPSTER, J. & HUTTER, O. F. (1984). Inward rectifier current noise in frog skeletal muscle. *Journal of Physiology* **349**, 299–327.

FABIATO, A. & FABIATO, F. (1979). Calculator programs for computing the composition of the solutions containing multiple metals and ligands used for experiments in skinned muscle cells. *Journal de Physiologie* **75**, 463–505.

FRANKENHAEUSER, B. & MOORE, L. E. (1963). The effect of temperature on the sodium and potassium permeability changes in myelinated nerve fibres of *Xenopus laevis*. *Journal of Physiology* **169**, 431–437.

GUPTA, R. K., GUPTA, P. & MORRE, R. D. (1984). NMR studies of intracellular metal ions in intact cells and tissues. *Annual Reviews of Biophysics and Bioengineering* **13**, 221–246.

HAGIWARA, S., MIYAZAKI, S. & ROSENTHAL, N. P. (1976). Potassium current and the effect of cesium on this current during anomalous rectification of the egg cell membrane of a starfish. *Journal of General Physiology* **67**, 621–638.

HAGIWARA, S. & YOSHII, M. (1979). Effects of internal potassium and sodium on the anomalous rectification of the starfish egg as examined by internal perfusion. *Journal of Physiology* **292**, 251–265.

HAGIWARA, S. & YOSHII, M. (1980). Effect of temperature on the anomalous rectification of the membrane of the egg of the starfish, *Mediaster aequalis*. *Journal of Physiology* **307**, 517–527.

HESS, P., METZGER, P. & WEINGART, R. (1982). Free magnesium in sheep, ferret and frog striated muscle at rest measured with ion-selective micro-electrodes. *Journal of Physiology* **333**, 173–188.

HESTRIN, S. (1981). The interaction of potassium with the activation of anomalous rectification in frog muscle membrane. *Journal of Physiology* **317**, 497–508.

HIRAOKA, M. & KAWANO, S. (1989). Calcium-sensitive and insensitive transient outward current in rabbit ventricular myocytes. *Journal of Physiology* **410**, 187–212.

HODGKIN, A. L., HUXLEY, A. F. & KATZ, B. (1952). Measurement of current–voltage relations in the membrane of the giant axon of *Loligo*. *Journal of Physiology* **116**, 424–448.

HODGKIN, A. L. & RUSHTON, W. A. H. (1946). The electrical constants of a crustacean nerve fibre. *Proceedings of the Royal Society* B **133**, 444–479.

HORIE, M. & IRISAWA, H. (1987). Rectification of muscarinic K^+ current by magnesium ion in guinea pig atrial cells. *American Journal of Physiology* **253**, H210–214.

HORIE, M. & IRISAWA, H. (1989). Dual effects of intracellular magnesium on muscarinic potassium channel current in single guinea-pig atrial cells. *Journal of Physiology* **408**, 313–332.

HORIE, M., IRISAWA, H. & NOMA, A. (1987). Voltage-dependent magnesium block of adenosine-triphosphate-sensitive potassium channel in guinea-pig ventricular cells. *Journal of Physiology* **387**, 251–272.

IMOTO, Y., EHARA, T. & GOTO, M. (1985). Calcium channel currents in isolated guinea-pig ventricular cells superfused with Ca-free EGTA solution. *Japanese Journal of Physiology* **35**, 917–932.

ISENBERG, G. (1976). Cardiac Purkinje fibers: Cesium as a tool to block inward rectifying potassium currents. *Pflügers Archiv* **365**, 99–106.

ISENBERG, G. & KLÖCKNER, U. (1982). Calcium tolerant ventricular myocytes prepared by preincubation in a 'KB medium'. *Pflügers Archiv* **395**, 6–18.

JOSEPHSON, I. R., SANCHEZ-CHAPULA, J. & BROWN, A. M. (1984). Early outward current in rat single ventricular cells. *Circulation Research* **54**, 157–162.

KURACHI, Y. (1985). Voltage-dependent activation of the inward-rectifier potassium channel in the ventricular cell membrane of guinea-pig heart. *Journal of Physiology* **366**, 365–385.

LEECH, C. A. & STANFIELD, P. R. (1981). Inward rectification in frog skeletal muscle fibres and its dependence on membrane potential and external potassium. *Journal of Physiology* **319**, 295–309.

MATSUDA, H. (1988). Open-state substructure of inwardly rectifying potassium channels revealed by magnesium block in guinea-pig heart cells. *Journal of Physiology* **397**, 237–258.

MATSUDA, H. & NOMA, A. (1984). Isolation of calcium current and its sensitivity to monovalent cations in dialysed ventricular cells of guinea-pig. *Journal of Physiology* **357**, 553–573.

MATSUDA, H., SAIGUSA, A. & IRISAWA, H. (1987). Ohmic conductance through the inwardly rectifying K channel and blocking by internal Mg^{2+}. *Nature* **325**, 156–159.

MITSUIYE, T. & NOMA, A. (1987). A new oil-gap method for internal perfusion and voltage clamp of single cardiac cells. *Pflügers Archiv* **410**, 7–14.

NAKAYAMA, T. & IRISAWA, H. (1985). Transient outward current carried by potassium and sodium in quiescent atrioventricular node cells of rabbits. *Circulation Research* **57**, 65–73.

OHMORI, H. (1978). Inactivation kinetics and steady-state noise in the anomalous rectifier of tunicate egg cell membranes. *Journal of Physiology* **281**, 77–99.

POWELL, T., TERRAR, D. A. & TWIST, V. W. (1980). Electrical properties of individual cells isolated from adult rat ventricular myocardium. *Journal of Physiology* **302**, 131–153.

SAIGUSA, A. & MATSUDA, H. (1988). Outward currents through the inwardly rectifying potassium channel of guinea-pig ventricular cells. *Japanese Journal of Physiology* **38**, 77–91.

SAKMANN, B. & TRUBE, G. (1984*a*). Voltage-dependent inactivation of inward-rectifying single-channel currents in the guinea-pig cell membrane. *Journal of Physiology* **347**, 659–683.

SAKMANN, B. & TRUBE, G. (1984*b*). Conductance properties of single inwardly rectifying potassium channels in ventricular cells from guinea-pig heart. *Journal of Physiology* **347**, 641–657.

VANDENBERG, C. A. (1987). Inward rectification of a potassium channel in cardiac ventricular cells depends on internal magnesium ions. *Proceedings of the National Academy of Sciences of the USA* **84**, 2560–2564.